Spring 5-2018

Pro-antimicrobial Networks Prepared via Degradable Thiol-ene Acetal Photopolymerization

Sarah Swilley
University of Southern Mississippi

The University of Southern Mississippi

Pro-antimicrobial Networks Prepared via Degradable Thiol-ene Acetal Photopolymerization

by

Sarah Swilley

A Thesis
Submitted to the Honors College of
The University of Southern Mississippi
in Partial Fulfillment
of the Requirement for the Degree of
Bachelor of Science
in the Department of Polymer Science and Engineering

May 2018

Approved by:

_____

Dr. Derek Patton, Ph.D., Thesis Adviser
School of Polymer Science and Engineering

_____

Jeffrey Wiggins, Ph.D., Director
School of Polymer Science and Engineering

_____

Ellen Weinauer, Ph.D., Dean
Honors College

Abstract

A degradable, antimicrobial polymer network with acetal crosslink junctions derived from *p*-anisaldehyde (pA), a common constituent found in star anise extract, is reported. The *p*-anisaldehyde was converted into a bis-functional acetal alkene monomer, which serves as a pro-antimicrobial form of the active aldehyde and a building block for materials referred to as pro-antimicrobial polymer networks via degradable acetals (PANDAs). Subsequently, the bis-functional acetal alkene monomer was photopolymerized with a multifunctional thiol to yield a thiol-ene network. PANDAs exhibit surface erosion behavior and yield sustained release of pA over 38 days when exposed to neutral or biologically relevant conditions. The pA released from PANDAs was shown to be effective against bacterial pathogens, including *Escherichia coli*, *Staphylococcus aureus*, *Salmonella enterica* serovar Typhi, and *Pseudomonas aeruginosa*. The result from this thesis points to promising routes for the design of completely degradable antimicrobial systems exhibiting sustained-release profiles with potential applications in pharmaceuticals, cosmetics, food packaging, and agriculture industries.

Keywords: thiol-ene, pro-antimicrobial, sustained-release, essential oils

Dedication

To my parents, Leslie and Robert Swilley, my siblings, Kate Speer and Dalton Swilley, and my dog, Tofu: my undergraduate career would not have been possible without your constant love and support. To my best friends, Kathleen Dixon and Michael Sanchez, thank you for keeping me sane throughout these last four years. To my fellow polymer science majors: I would not have succeeded in this program without each and every person in the graduating class of 2018. To my graduate students Doug and Dahlia Amato: thank you for pushing me to be the best scientist I could be; my dreams and accomplishments are largely thanks to you. Finally, to Dr. Patton: thank you for giving me the opportunity to work in your lab and become the scientist that I am today.

Acknowledgements

I would like to acknowledge my graduate students, Douglas V. Amato and Dahlia N. Amato; my fellow undergraduate researchers, William B. Martin, and Michael J. Sandoz; our collaborators, Logan Blancett, Olga V. Mavrodi, Glen Shearer, and Dmitri V. Mavrodi; and Derek L. Patton, my research adviser. The National Science Foundation (CHE-1710589 and OIA-1430364) for partial support of this research. Mississippi INBRE, funded by an Institutional Development Award (IDeA) from the National Institute of General Medical Sciences of the National Institutes of Health (8 P20 GM103476-11), and NCRR (5P20RR-016476-11). Lastly, Bruno Bock for the donation of PETMP.

Table of Contents

List of Illustrations

List of Schemes

List of Equations

List of Abbreviations

CFU	Colony Forming Units
DCM	Dichloromethane
DMA	Dynamic Mechanical Analysis
EOs	Essential Oils
MHA	Mueller Hinton II Agar
MHB	Mueller Hinton II Broth
NMR	Nuclear Magnetic Resonance spectroscopy
pAA	*Para*-anisaldehyde acetal
pA	*Para*-anisaldehyde
PANDA	Pro-Antimicrobial Network via Degradable Acetal
PETMP	Pentaerythritol Tetra(3-mercaptopropionate)
RT-FTIR	Real Time – Fourier Transform Infrared spectroscopy
SH	Thiol
TEM	Transmission Electron Microscopy
T_g	Glass transition temperature
TMSOTf	Trimethylsilyl trifluoromethanesulfonate
ZOI	Zone of Inhibition

Chapter I: Introduction

Antimicrobial resistance is an escalating crisis that threatens the sustainability of public health and agricultural ecosystems – a crisis that serves as the source of 700,000 deaths around the world on an annual basis.[1] As antibiotic effectiveness declines precipitously, a growing awareness of natural, plant-derived antimicrobial constituents has proliferated. Essential oils (EOs) are plant extracts that contain antimicrobial terpenes, aldehydes, and terpenoids. EOs have emerged as an effective alternative to antibiotics in fighting pathogenic microorganisms.[2-3] However, EOs exhibit low water solubility, high volatility, and are often chemically unstable; these challenges make practical applications of EOs difficult. Many strategies have been reported for encapsulation of EOs within films and colloidal systems;[4-5] however, deficiencies in these strategies are often observed, including low EO loading, poor EO encapsulation efficiencies, requirements for organic processing solvents, and uncontrolled release profiles.[6]

The work described in this thesis project involves the synthesis of new acetal containing monomers derived from intrinsically antimicrobial benzaldehydes, such as p-chlorobenzaldehyde, which have been previously studied by members of the Patton research group.[7] This project, however, focuses specifically on the synthesis and incorporation of *p*-anisaldehyde acetal monomer within a pro-antimicrobial thiol-ene network. Pro-antimicrobial networks, in this case, refer to polymeric networks that undergo degradation in neutral or mild acidic conditions and release active antimicrobial aldehydes. Photopolymerization kinetics, degradation and release kinetics, and the antimicrobial efficacy of both the monomer and corresponding networks were investigated.

Chapter II: Literature Review

2.1 Antibiotic Resistance

From the discovery of penicillin in 1928, to some of the most advanced medical discoveries of the 20th century, our society has heavily relied on the development of new antimicrobial compounds to remedy infections. However, pathogenic microbes are continually evolving, rendering the medicines used to treat infections caused by these pathogens ineffective. Over the last few years, the number of antibiotic discoveries has declined and simultaneously there has been an over-prescription of existing antibiotics. From 2000-2010 there has been a 40% increase of antibiotics globally in hospitals.[1] This overuse partially stems from the fact that many areas have access to over the counter and without prescription antibiotics; further, there has been an increase in counterfeit and sub-standard antibiotics on the market in various regions.[1]

Patients infected by drug resistant strains of bacteria suffer from a higher death rate, and a larger hospital bill. Methicillin-resistant strains of bacteria refer to any bacteria resistant to both penicillin and cephalosporin drug classes. In Europe, greater than 10% of *staphylococcus aureus* infections stem from methicillin-resistant *staphylococcus aureus* (MRSA).[1] Similarly, foodborne illnesses are also a problem. Around 30% of the population in industrialized countries will contract a food borne illness each year, some of which are caused by antibiotic resistant strains of bacteria; two million people died from a diarrheal disease in the year 2000.[2] Poorer communities suffer from drug resistant tuberculosis (TB), of which 480,000 new cases of resistant TB were reported in 2013; malaria, and Human Immunodeficiency Virus (HIV) that eventually causes the disease AIDS, also affect a large number of these populations.[1] Immunosuppressed patients, such as those infected with

HIV, or people who have recently undergone organ or bone marrow transplants, are more likely to contract bacterial infections.[8] Pathogen transmission is an issue, especially with bacteria, as they share genetic information, creating new drug resistant forms of themselves. International travel allows these pathogens to travel worldwide, thus creating a global crises. Studies by O'Neil have projected that, if left untreated, by 2050, 10 million people would die globally due to drug resistance.[1] Further, 10 trillion USD will be spent yearly to tackle infections arising from these "superbugs". Undoubtedly, these untreatable infections will result in global suffering if actions are not implemented to effectively mitigate the spread of antibiotic-resistant pathogens.[1]

2.2 Essential Oils as Antimicrobials

As our strongest antibiotics lose efficacy, scientists have turned to nature as an alternative source for antimicrobial compounds. Essential oils (EOs), or extracts derived from plants, have been used throughout history to combat a variety of infections. The desired effect of these EOs is directly related to the functional groups present within the constituents of the oil. Different functionalities such as alcohols, aldehydes, esters, ketones and phenols present in the constituents linalool (flowers), citronellal (citrus), carvone (spearmint/dill), and carvacrol (oregano), respectively, give rise to various antimicrobial effects.[9] Current research has shown that EOs also exhibit antiviral, antimycotic, antitoxigenic, antiparasitic, and insecticidal properties.[2] The antimicrobial properties of EOs can be attributed to a variety of mechanisms. For example, the hydrophobic nature of EOs enables them to partition within the lipids of the bacterial cell membrane rendering the membrane more permeable.[2] The increased permeation leads to leakage of the contents from the cell, resulting in cell death. Phenolic EOs such as carvacrol are thought to disrupt

the proton motive force, electron flow, and active transport, and cause coagulation of the cell contents, leading to cell death.[2]

Inouye and coworkers effectively demonstrated the capability of aldehyde-containing constituents to kill various strains of bacteria. Their study focused on comparing the effectiveness of different functionalities against gram-positive and gram-negative bacteria. Phenolics, terpenes, aldehydes, terpene ketones, and esters were examined. The aldehyde-containing constituents used were citral, octanal, and nonanal (all found in citrus), cinnamaldehyde (cinnamon), and perillaldehyde (perilla herb). Their results showed that constituents containing aldehydes or phenols are the most active against bacteria, and all others were significantly weaker.[10]

Potential applications include food packaging in which bacteria such as *Salmonella, E. coli,* and *L. monocytogenes* are an issue. EOs have been incorporated directly into foods or food packaging materials to increase the shelf life of products that are prone to spoilage. One important requirement within the food packaging industry is that the concentration of EO must be high enough to exert antimicrobial effects while not altering the flavor of the food.[2]

2.3 Encapsulating Essential Oils

Polymer nanoparticles have been utilized in pharmaceutical, biomedical, and cosmetic industries. These particles have gained attention due to their ability to protect bioactive compounds, such as EOs or other drugs, from sources that initiate degradation: light, heat and oxygen. Nanoparticles also act as a carrier, delivering active drugs to their targets; this allows for better bioavailability of hydrophobic drugs. Similarly, they can result in a prolonged release within the therapeutic window. Many methods for

encapsulating EOs within polymeric particles have been reported, such as nanoprecipitation, coacervation, spray drying, rapid expansion of supercritical solutions, and most commonly, encapsulation within solid lipid nanoparticles.[6] While these strategies have their benefits, many of them suffer from multiple issues such as poor encapsulation efficiencies or substandard release profiles. For example, when thymol, carvacrol and cholesterol were encapsulated within multilamellar vesicles and dried of solvent, a 4.16% encapsulation efficiency was observed.[4] Recently, Gomes et al. encapsulated both eugenol and trans-cinnamaldehyde within degradable poly(lactic-co-glycolic acid) (PLGA) matrix particles, and observed an initial burst release followed by a slower rate of release of the antimicrobial EOs.[11] Organic solvents were used during the encapsulation process which is non-ideal as residual solvent could remain after the particles are formed. Keawchaoon and coworkers encapsulated carvacrol within chitosan nanoparticles and found that the release of carvacrol plateaued within 30 days, releasing 23% in phosphate buffer saline at pH = 7.[12-13] The poor release profile suggests that further improvements in encapsulation efficiency and controlled release kinetics of EOs from matrices are desired.

Acetal functionalized polymer networks have been utilized by multiple research groups, as acetals readily degrade at biological pH.[14] Linear polyacetals, such as those synthesized by Heller et al. degrade into non-toxic products and that these polymers show no preferential accumulation in the major organs.[15] The Fréchet group demonstrated the ability to produce protein-loaded microparticles using acetals as cross-linkers.[16] Benzaldehyde acetal was chosen as the cross-linker to control the degradation rate of the polymer by changing the *para* position on the molecule. In their specific study, it was shown that *p*-methoxy substituted benzaldehyde had a half-life of 24 hours at pH 7.4.[14]

Recently, we published a paper describing the use of p-chlorobenzaldehyde derived pro-antimicrobial networks.[7] Real-time Fourier transform infrared spectroscopy revealed that thiol-ene networks achieved over 95% conversion between thiol and alkene functionalities. Kinetic release studies, such as the one described in this thesis, showed gradual release of p-chlorobenzaldehyde over 120 hours (>70% released). The antimicrobial activity of the pro-antimicrobial network was shown to be effective for both gram-positive (*Bacillus subtilis and S. aureus*) and gram-negative (*E. coli, P. aeruginosa and Burkholderia cenocepacia*) bacteria with killing efficiency over 99.5% within 24 hours. These acetal-based thiol-ene networks represent a new approach to afford high loading and a controlled release of antimicrobial agent from crosslinked polymeric networks.

2.4 Research Overview

Building on our previous efforts employing p-chlorobenzaldehyde as the active building block for pro-antimicrobial networks via degradable acetals (PANDAs), the work in this thesis shifts focus away from oil derived compounds for network building blocks towards bio-based aldehydes found in nature to offer a fully degradable antimicrobial system based on essential oils. Herein, we employed *p*-anisaldehyde (pA), an extract from star anise (*Pimpinella anisum)* seeds, to fabricate a new class of antimicrobial PANDAs using thiol-ene photopolymerization. The networks that are derived from *p*-anisaldehyde completely degrade when exposed to humid or acidic environments, and upon degradation release the active form of the EO into the surrounding environment. We demonstrate that incorporation and subsequent release of pA from a PANDA exhibits potent antimicrobial

activity against a variety of clinically relevant pathogens. The contents of this thesis were published as a 2018 peer-reviewed journal article in Acta Biomaterialia.[17]

Chapter III: Materials and Methods

3.1 Materials

The chemicals *p*-anisaldehyde (pA), trimethylol propane diallyl ether, 2-hydroxy-2-methylpropiophenone (Darocur 1173), trimethylsilyl trifluoromethanesulfonate (TMSOTf), dichloromethane (DCM), allyloxytrimethylsilane, pyridine, sodium bicarbonate, diethyl ether, magnesium sulfate ($MgSO_4$), dextrose, 2,3,5,6-tetrachloronitrobenzene, 3-(4,5-dimethylthiazol-2-yl)-2,5-diphenyltetrazolium bromide (MTT), hexane, 0.5 M Tris-HCl in H_2O, acetonitrile-d_3, Aqua Dead Cell Stain™, LIVE/DEAD BacLight Bacterial Viability Kit staining kit, BacLight RedoxSensor CTC Vitality Kit and ethyl acetate were acquired from Thermo Fisher Scientific. Pentaerythritol tetra(3-mercaptopropionate) (PETMP) was provided by Bruno Bock. Difco Agar, yeast extract, Bacto Tryptone, Mueller Hinton broth and agar, were from Becton, Dickinson and Company. Ham's F-12 and trypsin-EDTA were obtained from GIBCO. Hemin chloride (type II), protoporphyrin IX, histidine (free base), proline, 37% formaldehyde in H_2O, dimethyl sulfoxide (DMSO), fluconazole, fetal bovine serum (FBS), Dulbecco's Modified Eagle's Medium (DMEM) and N-2-hydroxyethylpiperazine-N'-2-ethanesulfonic acid (HEPES) was purchased from Sigma Aldrich. All the materials were obtained at the highest purity available and used without further purification unless otherwise specified.

3.2. Characterization Methods.

A Bruker Ascend 600 MHz (TopSpin 3.5) spectrometer was used to record $^{1}H/^{13}C$ NMR spectra with either chloroform-*d* or acetonitrile-d_3. High resolution mass

spectroscopy (HRMS) was performed with positive electrospray ionization on a Bruker 12 Tesla APEX-Qe FTICR-MS with an Apollo II ion source. Dynamic mechanical analysis (DMA) was performed using a TA Instruments Q800 dynamic mechanical analyzer in tension mode equipped with a gas cooling accessory. Samples were clamped, evaluated at a strain of 1 %, and heated from -80 °C to 80 °C at a ramp rate of 3 °C min^{-1}. Kinetic data was obtained using real-time FTIR (RT-FTIR) spectroscopy by determining the conversions of the thiol and ene functional groups. The RT-FTIR studies were conducted using a Nicolet 8700 FTIR spectrometer with a KBr beam splitter and a MCT/A detector with a 320–500 nm filtered ultraviolet light source. Each sample was exposed to UV light with an intensity of 400 mW cm^{-2}. Series scans were recorded, where spectra were taken approximately 2 scans s^{-1} with a resolution of 4 cm^{-1}. Thiol conversion was monitored via integration of the SH peak between 2500-2620 cm^{-1} while the conversion of the alkene was monitored between 3050-3125 cm^{-1}. Optical density (OD) and fluorescence readings were performed in a BioTek Synergy 2 programmable microplate reader (BioTek Instruments).

3.3 Synthesis and Characterization of Monomer

The procedure of Noyori et al. [18] was modified to synthesize *p*-anisaldehyde acetal (pAA) monomer (Scheme 1). A 250-mL round bottom flask was flame dried and equipped with a stir bar. Trimethylsilyl trifluoromethanesulfonate (TMSOTf, 200 mL) was added to the round bottom flask along with 20 mL of dichloromethane (DCM) under a nitrogen atmosphere at -84°C. Allyloxytrimethylsilane (37 mL, 208 mmol), *p*-anisaldehyde (pA), 12g, 88 mmol), and 25 mL of DCM were mixed together and added dropwise to the round bottom; the reaction was stirred for 3 hours, warmed to -30°C and stirred for another hour. It was quenched with 15 mL of pyridine and then added to 100 mL of sodium bicarbonate

solution. The quenched reaction mixture was then extracted 3 times with 100 mL of diethyl ether and dried with $MgSO_4$. The solvent was removed *in vacuo* and the resulting residue was purified via column chromatography using a 9:1 hexanes:ethyl acetate solvent mixture in order to remove any residual aldehyde. Purification yielded a clear oil (13.6 g, 65.9 % yield). ^{1}H NMR ($CDCl_3$) δ 7.45 (dd), 6.93 (dd), 5.97 (m), 5.62 (s), 5.35 (dd), 5.17 (dd), 4.07 (d), 3.82 (s). ^{13}C NMR ($CDCl_3$) δ 159.66, 134.16, 130.68, 127.97, 116.67, 113.52, 100.29, 66.00, and 55.22. HRMS (ESI^+) m/z calculated for $C_{14}H_{18}O_3$ $[M+Na]^+$ 257.114816; Found 257.114817.

3.4 Preparation of PANDA Disks

Disks were prepared by combining PETMP, pAA (molar ratio of SH:alkene of 1:1), and 4 weight % of Darocur 1173 (photoinitiator) in a 20 mL scintillation vial, then mixed thoroughly. The mixture, in different μL amounts (changed depending on the experiment the films were used for), were pipetted onto a glass slide, and then covered with another slide spaced with Teflon spacers. The samples were then cured using an Omnicure S1000-1B with a 100W mercury lamp (λmax = 365 nm, 320–500 nm filter) at an intensity of 400 mW cm^{-2} for 30 seconds on each side. Control disks were prepared in the same way, but with trimethylol propane diallyl ether (non-degradable) instead of pAA.

3.5 Degradation Studies

3.5.1 Optical Degradation

Surface erosion was monitored via optical microscopy. Both a PANDA film and a control film were prepared as stated above and placed in a 1 N HCl aqueous solution. Pictures were taken over the course of three hours, with one image per 5 minutes. To graph

the degradation over time, the remaining disk area, A_t, was plotted with respect to the initial area A_∞. These results were then fitted to the Hopfenberg model.[19]

3.5.2 Analysis of Degradation and Release via NMR

The release of pA over time was analyzed via NMR spectroscopy. 2,3,5,6-tetrachloronitrobenzene, used as an internal standard, was dissolved into 500 mL of deuterated acetonitrile. 125 mL of 100 mM Tris-HCl buffer, pH 7.4, was then mixed in; the resulting solution was added to an NMR tube containing a 5 mL PANDA disk, and flame sealed. The proton connected to the aldehyde results in a peak around 10 ppm, and this was integrated with respect to the internal standard to determine the concentration of pA in solution over a period of 38 days.

3.6 Antimicrobial Assays

3.6.1 Zone of Inhibition

The antimicrobial activity of PANDA disks was tested against several species of bacteria via the zone of inhibition (ZOI) method. The indicator microorganisms included Escherichia coli ATCC 43895 (serotype O157:H7), *Staphylococcus aureus* RN6390, *Salmonella enterica serovar Typhi* ATCC 6539 (*Sal. Typhi*), and *Pseudomonas aeruginosa* PAO1. The testing was done on Mueller Hinton II agar (MHA) plates that have been overlaid with soft agar seeded with individual bacterial strains. The soft agar contained (per liter): 10 g of Bacto Tryptone, 6 g of Difco agar, and 8 g of sodium chloride. To create an overlay, the indicator organisms were grown overnight at 37 °C in Mueller Hinton II broth (MHB). The overnight cultures were diluted 1:5 with fresh MHB, and mixed with molten soft agar to achieve a ~10^8 CFU mL^{-C} density. From this mixture, 4 mL aliquots were overlaid onto MHA base plates and allowed to completely solidify. After solidification of

the soft agar, 50 mm^3 disks were overlaid on the plates and incubated at 37 °C. The zones of inhibition (ZOI) were measured after 24 h and reported as the distance from the edge of the disk to the edge of the zone. Three replicates were carried out for each disk/bacterial strain, with the mean and standard deviation reported (experiment was repeated twice).

3.6.2 Minimum Inhibitory Assay

A modified broth macrodilution method was used to determine the minimum size of PANDA disks needed to inhibit bacterial growth. Briefly, overnight bacterial cultures in MHB were adjusted to ~10^5 CFU mL^{-1}. PANDA disks of different sizes (5-100 mm^3) were added to 4 mL of bacterial cultures. The tubes were then incubated at 37 °C and shaken at 200 rpm for 24 h. Bacteria suspended in MHB served as a positive control, while MHB without bacterial inoculum served as a negative control. The inoculated tubes were assessed by measuring optical density at 600 nm after 24 h, where OD < 0.05 was considered negative for bacterial growth. Three replicates were carried out for each disk size and bacterial strain, with the mean and standard deviation reported (experiment repeated twice).

3.7 Cell Membrane Integrity

3.7.1 LIVE/DEAD Staining

A LIVE/DEAD BacLight Bacterial Viability Kit was used to probe the cell membrane integrity of the chosen bacteria. *P. aeruginosa* was diluted to 10^5 CFU/mL, and 4 mL of this suspension was exposed to a 100 mm^3 PANDA film. This was then incubated at 37°C while shaken at 200 rpm. A 100-mL aliquot was removed at 0 h and 30 h, and these aliquots were placed into a Corning 96-well solid black microplate and then mixed with 100 mL of LIVE/DEAD staining agent. They were then incubated, in the dark, for 15

minutes before the fluorescence was measured with a 528/20 nm excitation filter for the SYTO9 indicator, a 620/40 nm filter for the propidium iodide indicator, and 485/20 nm excitation filter for both indicators. Confocal imaging was completed by applying 5 mL of the stained samples onto microscope slides. The samples were assayed in triplicate and the experiment was repeated twice.

3.7.2 TEM Imaging

Transmission electron micrographs of the bacterial suspensions prepared as described in section 3.6.1 were taken with a Zeiss 900 electron microscope operating at 50 kV and outfitted with a Model 785 Erlangshen ES1000 WCCD camera (Gatan). Samples were applied to 200 mesh copper grids (3.05 mm, 200 lines per inch square mesh, Electron Microscopy Sciences) coated with Formvar (5% polyvinyl formal resin).

Chapter IV: Results and Discussion

4.1 Synthesis and Characterization of Monomer

Scheme 1A shows the synthetic scheme for the preparation of pAA, which was produced with a yield of 66% after purification. The resulting monomer was characterized via ^{1}H NMR spectroscopy (Figure 1); peak assignments were in good agreement with values reported in the literature.[18] To investigate the antimicrobial properties of the pAA and pA monomers, 10 µL of pure pAA and pA were plated on agar and overlaid with *Sal. Typhi* (Scheme 1A).

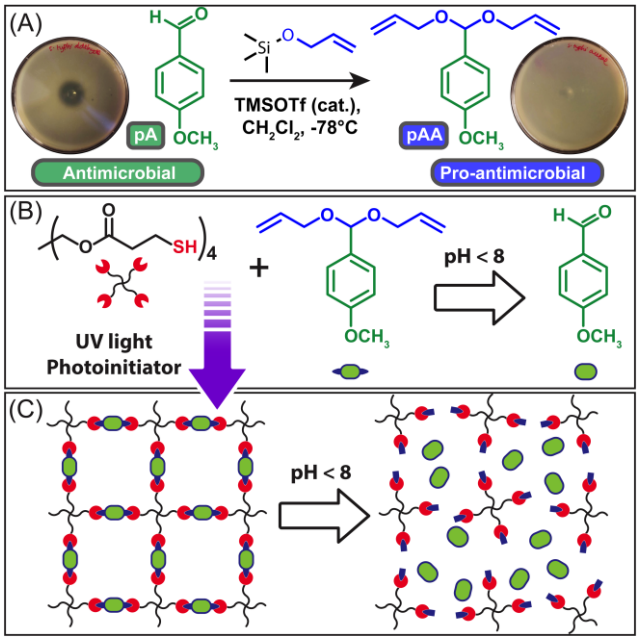

Scheme 1: Synthesis, photopolymerization, and degradation scheme.

Following an incubation period of 24 h, pAA showed no visible zone of inhibition indicating the acetal form of the monomer is not an active antimicrobial compound. In contrast, pA showed a 1 cm zone of inhibition. These results indicate that pAA functions as a pro-antimicrobial compound exhibiting antimicrobial activity only upon hydrolysis back to the benzaldehyde.

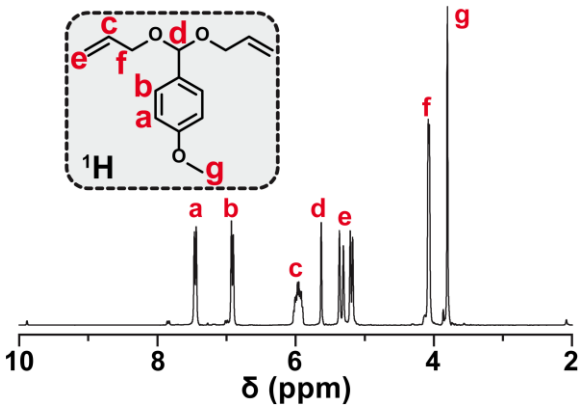

Figure 1: NMR spectra of monomer.

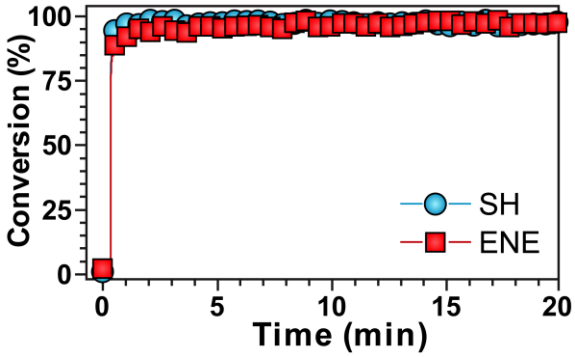

Figure 2: Conversion between thiol and alkene monomers

4.2 Photopolymerization and Characterization of Polymer Films

PANDA films were fabricated via radical-mediated step-growth thiol-ene photopolymerization (Scheme 1B) using pentaerythritol tetrakis(3-mercaptopropionate) (PETMP) and pAA as monomers. PETMP and pAA were copolymerized using a 1:1 alkene/thiol mole stoichiometry. Upon polymerization, the composition of the PANDA films is 47 wt.% pAA, which translates to pA loading of 27 wt.%. The photopolymerization kinetics, when conducted under a medium pressure UV light (400 mW cm^{-2}), were rapid and exhibited nearly quantitative conversion (>95%, Fig. 2) of both thiol and alkene functional groups in less than 60 s. The step-growth polymerization mechanism observed for

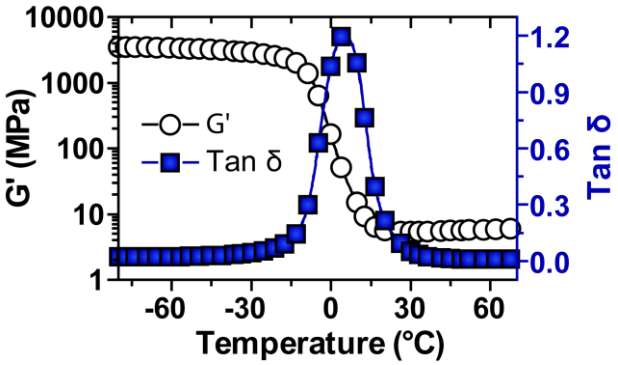

Figure 3. Dynamic mechanical analysis of PANDA films.

radical-mediated thiol-ene polymerization of PETMP and pAA ensures that each crosslink junction contains a hydrolytically cleavable acetal linkage for the release of pA from the network (Scheme 1C). Additionally, the resulting PANDAs possess a narrow tan δ (indicative of a homogenous network), a glass transition temperature of -0.5 °C (Fig. 3) and are optically transparent – typical of thiol-ene materials.

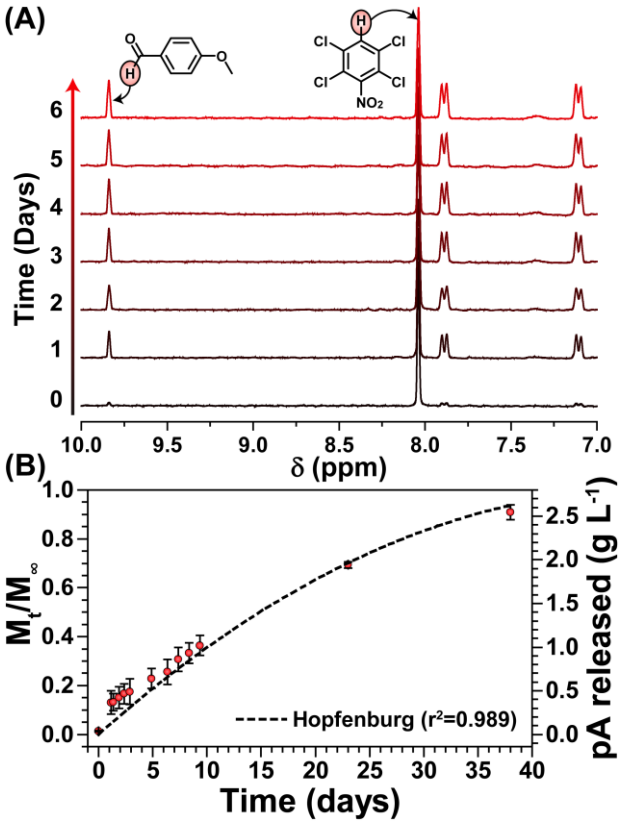

Figure 4. (A) NMR spectra of degradation products (B) Release of aldehyde and corresponding fit to Hopfenburg model.

4.3 Degradation Studies

The PANDA degradation and pA release kinetics were initially characterized using ^{1}H NMR spectroscopy. The kinetic experiment was conducted over 38 days at pH 7.4 by inserting disks in acetonitrile-d_3/buffer solutions in sealed NMR tubes. 2,3,5,6-tetrachloronitrobenzene (δ = 7.75 ppm) was employed as an internal standard enabling integration relative to the benzylic aldehyde proton (δ = 9.85 ppm) to determine time-resolved pA concentration (Fig. 4A). The release profile of pA obtained from the integrated ^{1}H NMR data is shown in Figure 4B. At pH 7.4, an initial burst release was not observed; however, a slow release profile was observed where 90% pA was released within 38 days. To better quantify

$$\frac{M_t}{M_\infty} = 1 - \left[1 - \frac{k_0 t}{C_0 a}\right]^2$$

Equation 1: Hopfenberg Model

the release data, the release profile was fit to the cylindrical Hopfenberg model [19] described in Equation 1:

where, M_t is the concentration of released pA at time *t*, M_∞ is the theoretical maximum of pA released, k_0 is the erosion rate constant, C_0 is the initial concentration of drug in the matrix, and *a* is the initial radius of the cylinder. The half-life of the PANDA degradation was determined to be 14.9 days from the Hopfenberg model. To investigate the process of erosion for the PANDA disks over time, PANDA disks and non-degradable control disks (trimethylolpropane diallyl ether and PETMP) were fabricated, submerged in a 1N aqueous HCl solution, and imaged using optical microscopy over time. The optical images from the accelerated degradation experiment are shown in Figure 5A. Within 1 h, significant surface erosion was observed. The low solubility of the *p*-anisaldehyde and tetrafunctional alcohol (degradation products) in water results in the solid disk degrading to an oil-like residue within 3 h. The area of the degradation front, as highlighted by the green arrows in Figure 5A, was used to quantify the degradation process under low pH conditions. A plot of the remaining disk area at time *t* (A_t) relative to the initial area (A_∞) was plotted over time and then fit to the Hopfenberg model, where M_t/M_∞ were replaced by A_t/A_∞. The degradation at pH 0.1 was 380x faster (half-life = 0.04 days) – much faster than expected when compared to the degradation at pH 7.4 observed by

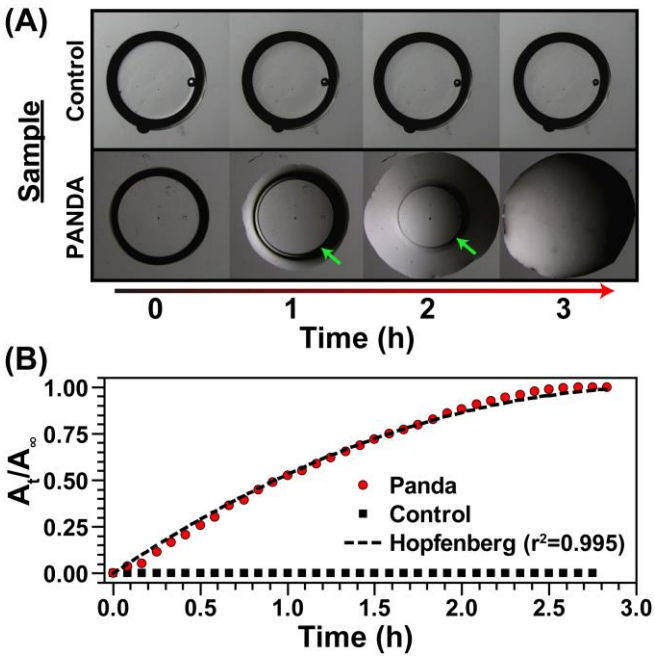

Figure 5. (A) Visual degradation of PANDA films in 1 N HCl (B) Plotted degradation fit to Hopfenberg model

NMR. The results from these collective degradation studies are consistent with acid sensitive hydrolysis behavior of acetals.[15]

4.4 Antimicrobial Assays

4.4.1 Zone of Inhibition

The antimicrobial activity of both PANDA disks and control disks was initially evaluated via a ZOI assay using clinically isolated strains: *S. aureus* RN6390 and *P. aeruginosa* PAO1, and foodborne pathogens: *E. coli* ATCC 43895 (serotype O157:H7) and *Sal. Typhi* ATCC 6539 (Fig. 6). As expected, control disks without *p*-anisaldehyde showed no antimicrobial activity for any bacteria in the ZOI experiments. However, ZOIs greater than 1 cm were observed for the PANDA disks, where larger ZOI values indicate more potent inhibition of the bacteria. The ZOI assay showed that the order of antimicrobial inhibition was *Sal. Typhi* > *S. aureus* > *E. coli* O157:H7 > *P. aeruginosa*.

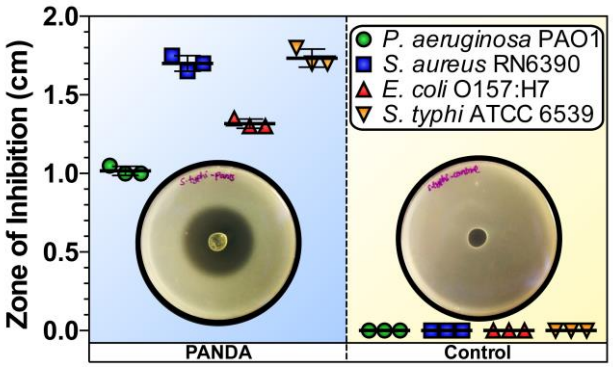

Figure 6. Zone of inhibition for PANDA and control disks. Plotted data points represent individual measurements.

4.4.2 Minimum Inhibition Assay

To determine the PANDA disk size required to inhibit bacterial growth, a minimum inhibitory disk size assay was performed with bacteria in their exponential growth phase (10^5 CFU mL^{-1} in 4 mL media). The bacteria were challenged with PANDA disks (0-100 mm^3). Note, larger disk size translates to a higher pA concentration released at a given time point. The minimum inhibition assay, as presented in Figure 6, showed that inhibition of bacteria increased with an increase in disk size, and 100 mm^3 (910 mg/mL pA) disks

effectively inhibited all strains of bacteria tested. An optical density reading of <0.05 is considered negative for bacterial growth under these experimental conditions. *E. coli* O157:H7 and *P. aeruginosa* required the largest disk size, however, *Sal. Typhi* and *S. aureus* were inhibited by 50 mm^3 disks (455 mg/mL pA). The concentration of pA released was estimated from the NMR release profile previously described.

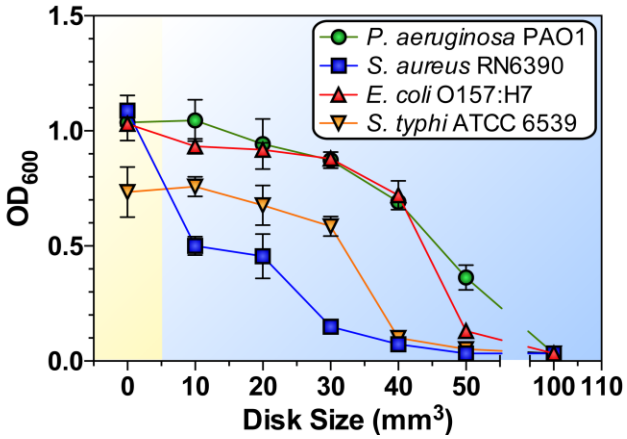

Figure 7. Minimum inhibition assay of different sized PANDA disks.

4.5 Cell Membrane Integrity

To investigate the possible mode of action for pA antimicrobial activity, the cell membrane integrity was analyzed for *P. aeruginosa* via a LIVE/DEAD staining – a method that was supported by TEM imaging. SYTO9 is capable of penetrating healthy cell membranes, and results in a green fluorescence; while propidium iodide only enters cells with damaged cell membranes resulting in red fluorescence. Figure 8A shows that at 0h of PANDA exposure the *P. aeruginosa* fluoresced green while after 30 h the sample fluoresced red, indicating damaged cell membranes. The disruption of the cell membrane was further concluded with the use of TEM imaging where in Figure 8D there is a clear disruption of the cell membrane as compared to the healthy bacteria in Figure 8C.

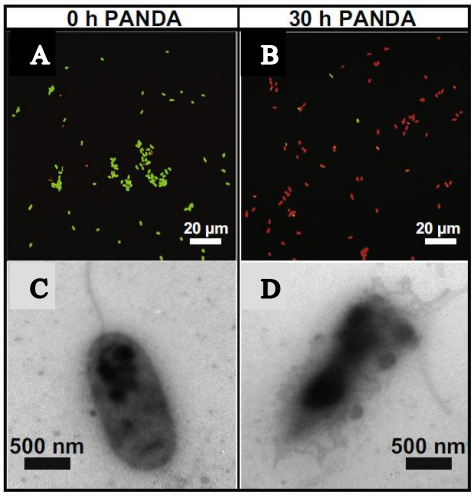

Figure 8. LIVE/DEAD staining images (A) at 0h (B) at 30 h; TEM images (C) at 0h and (D) at 30h

Chapter V: Conclusion

In this thesis, we have demonstrated a bactericidal, pro-antimicrobial network that is effective against both gram-positive and gram-negative bacteria. By using confocal microscopy and TEM imaging, we showed that these antimicrobial polymers mainly kill bacteria via membrane disruption. Due to the effectiveness of pA and PANDA networks, these types of polymers could potentially be utilized to combat bacteria in the medical field. We demonstrated a potent bio-based pro-antimicrobial polymer network that has the versatility to treat gram positive and gram negative bacterial pathogens through the sustained release of pA over time. Through a combination of confocal microscopy and transmission electron microscopy, we showed PANDAs primary mode of action is via membrane disruption. The design of the PANDA network combined with the potency of pA has the potential to part of the arsenal of defenses against a broad spectrum of pathogens and exhibits potential for future *in vivo* experiments.

References

1. O'Neil, J., *Antimicrobial Resistance: Tackling a Crisis for the Health and Wealth of Nations*. Wellcome and HM Government: London, 2016.
2. Burt, S., Essential oils: their antibacterial properties and potential applications in foods—a review. *Int. J. Food Microbiol.* **2004,** *94* (3), 223-253.
3. Nielsen, P. V.; Rios, R., Inhibition of fungal growth on bread by volatile components from spices and herbs, and the possible application in active packaging, with special emphasis on mustard essential oil. *Int. J. Food Microbiol.* **2000,** *60* (2), 219-229.
4. Asbahani, A. E.; Miladi, K.; Badri, W.; Sala, M.; Addi, E. H. A.; Casabianca, H.; Mousadik, A. E.; Hartmann, D.; Jilale, A.; Renaud, F. N. R.; Elaissari, A., Essential oils: From extraction to encapsulation. *Int. J. Pharm.* **2015,** *483* (1–2), 220-243.
5. Sánchez-González, L.; Vargas, M.; González-Martínez, C.; Chiralt, A.; Cháfer, M., Use of Essential Oils in Bioactive Edible Coatings: A Review. *Food. Eng. Rev.* **2011,** *3* (1), 1-16.
6. Majeed, H.; Bian, Y.-Y.; Ali, B.; Jamil, A.; Majeed, U.; Khan, Q. F.; Iqbal, K. J.; Shoemaker, C. F.; Fang, Z., Essential oil encapsulations: uses, procedures, and trends. *RSC Adv.* **2015,** *5* (72), 58449-58463.

7. Amato, D. N.; Amato, D. V.; Mavrodi, O. V.; Martin, W. B.; Swilley, S. N.; Parsons, K. H.; Mavrodi, D. V.; Patton, D. L., Pro-Antimicrobial Networks via Degradable Acetals (PANDAs) Using Thiol–Ene Photopolymerization. *ACS Macro Lett.* **2017,** *6* (2), 171-175.
8. White, T. C. M., K. A; Bowden, R. A., Clinical, cellular, and molecular factors that contribute to antifungal drug resistance. *Clinical Microbiology Reviews* **1998,** *11* (2), 382-402.
9. van Zyl, R. L. S., S. T; van Vuuren, S. F., The biological activities of 20 nature identical essential oil constituents. *J. Essent. Oil Res.* **2006,** *18*, 129-133.
10. Inouye, S. T., T; Yamaguchi, H., Antibacterial activity of essential oils and their major constituents against respiratory tract pathogens by gaseous contact. *Journal of Antimicrobial Chemotherapy* **2001,** *47* (5), 565-573.
11. Gomes, C.; Moreira, R. G.; Castell‐Perez, E., Poly (DL‐lactide‐co‐glycolide) (PLGA) Nanoparticles with Entrappedtrans‐Cinnamaldehyde and Eugenol for Antimicrobial Delivery Applications. *J. Food Sci.* **2011,** *76* (2), N16-N24.
12. Keawchaoon, L. Y., R., Preparation, characterization, and *in vitro* release study of carvacrol-loaded chitosan nanoparticles. *Colloids and Surfaces B: Biointerfaces* **2011,** *84*, 163-171.
13. Keawchaoon, L.; Yoksan, R., Preparation, characterization and in vitro release study of carvacrol-loaded chitosan nanoparticles. *Colloids and Surfaces B: Biointerfaces* **2011,** *84* (1), 163-171.
14. Binauld, S.; Stenzel, M. H., Acid-degradation polymers for drug delivery: a decade of innovation. *Chem. Commun.* **2013,** *49*, 2082-2102.
15. Heller, J., Poly (ortho esters). In *Biopolymers I*, Langer, R. S.; Peppas, N. A., Eds. Springer Berlin Heidelberg: Berlin, Heidelberg, 1993; pp 41-92.
16. Murthy, N.; Thng, Y. X.; Schuck, S.; Xu, M. C.; Fréchet, J. M. J., A Novel Strategy for Encapsulation and Release of Proteins: Hydrogels and Microgels with Acid-Labile Acetal Cross-Linkers. *J. Am. Chem. Soc.* **2002,** *124* (42), 12398-12399.
17. Amato, D. V.; Amato, D. N.; Blancett, L. T.; Mavrodi, O. V.; Martin, W. B.; Swilley, S. N.; Sandoz, M. J.; Shearer, G.; Mavrodi, D. V.; Patton, D. L., A bio-based pro-antimicrobial polymer network via degradable acetal linkages. *Acta Biomater.* **2018,** *67*, 196-205.
18. Tsunoda, T.; Suzuki, M.; Noyori, R., A facile procedure for acetalization under aprotic conditions. *Tetrahedron Lett.* **1980,** *21* (14), 1357-1358.
19. Hopfenberg, H. B., Controlled Release from Erodible Slabs, Cylinders, and Spheres. In *Controlled Release Polymeric Formulations*, AMERICAN CHEMICAL SOCIETY: 1976; Vol. 33, pp 26-32.